Article

Design, Synthesis, and Bioactivity of Chalcone Derivatives Containing Indanone

Nan Sun, Chenyu Gong, Yuanxiang Zhou, Yuanquan Zhang, Nian Zhang, Li Xing, and Wei Xue*

Read Online

ACCESS | Metrics & More | Article Recommendations | Supporting Information

ABSTRACT: A series of chalcone derivatives containing indanone were designed and synthesized by aldehyde-ketone condensation and etherification. The activity test demonstrated that the majority of the compounds had good therapeutic and protective activities against tobacco mosaic virus (TMV) at a concentration of 500 μg/mL when being tested. Among them, the target compounds **N2** and **N7** showed good therapeutic activities against TMV with EC_{50} values of 70.7 and 89.9 μg/mL, respectively, which were better than that of ningnanmycin (158.3 μg/mL). **N2** and **N10** showed better protective activities against TMV with EC_{50} values of 60.8 and 120.3 μg/mL, which were superior to that of ningnanmycin (175.6 μg/mL). A hydrogen bond interaction was observed between **N2** and ARG-341 with a bond length of 3.08 Å and a hydrogen bond was observed between ningnanmycin and ASP-66 with a bond length of 3.72 Å. In contrast, the hydrogen bond length of compound **N2** was shorter and its binding was closer. Meanwhile, when the heartleaf tobacco was being treated with **N2**, its increasing rate of malondialdehyde slowed and its content of defense enzymes significantly increased, again reflecting the good activity of **N2** against TMV.
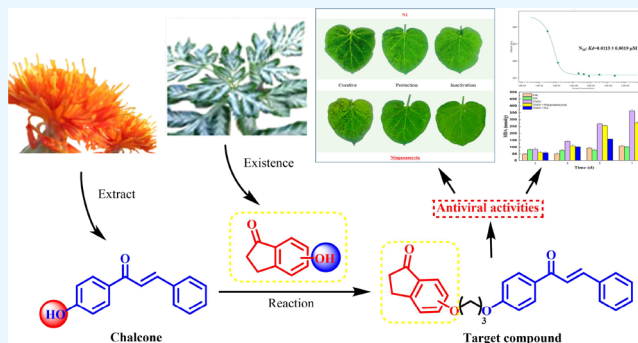
1. INTRODUCTION

In the absence of a plant-specific immune system, the parasitic effect of virus on its cells is tremendous, contributing to severe losses, and the prevention and treatment are difficult and complex. Thus, plant viruses are also called "cancer".[1] As an RNA virus, tobacco mosaic virus (TMV) has given rise to infections in 36 crops of the families of Amaranthaceae, Chenopodiaceae, Asteraceae, Cruciferae, and Solanaceae since its discovery, causing huge economic losses.[2] Through minor wounds and stomas, TMV destroys the chlorophyll in leaves, weakens photosynthesis, inhibits plant growth, and causes plant growth difficulties, dysplasia, deformity, and even death. At present, the main prevention and treatment have been achieved by means of antiviral agents that induce host defense responses,[3] such as ningnanmycin (NNM) and ribavirin. However, the long-term and large-scale use of traditional antiviral agents not only increases the drug resistance of pathogens but also brings a series of environmental issues, such as excessive pesticide residues and eutrophication.[4] Therefore, it is of great significance to explore and develop new antiviral agents with high efficiency, low toxicity, and environmental protection for the control of the tobacco mosaic disease.

Chalcone exists widely in licorice,[5] safflower,[6] oxytropis falcate bunge,[7] hops,[8] and other plants as an essential natural product and an important intermediate for the synthesis of flavonoids. Chalcone has a wide range of pharmacological activities, such as antibacterial,[9] antiviral,[10] insecticidal,[11] anti-inflammatory,[12] antitumor,[13] antioxidant,[14] and other biological activities,[15] due to its flexibility and ability to bind to a variety of receptors. In addition, chalcone contains α,β-unsaturated carbonyl groups in its structure, which can be conjugated with nucleophilic groups (such as sulfhydryl groups in proteins) in bacteria, viruses, and pests, thus causing them to die.[16]

Indanone also exists widely in the active molecules of natural products, drugs, and pesticides. To name only a few, 1-methoxy-6-methyl-3-oxo-2,3-dihydro-1*H*-4-aldehyde (**I**) and pterosin B (**II**) extracted from marine cyanobacteria and *Pteris ensiformis* are found to contain indanone structural units,[17,18] as shown in Figure 1. Indanones have antibacterial,[19] antiviral,[20] anti-Alzheimer's disease,[21] antitumor,[22] and other biological activities.[23] Some of them have been used in clinical practice. For example, donepezil (**III**),[24] an acetylcholinesterase inhibitor, has been approved by the United States Food and Drug Administration for the treatment of Alzheimer's disease.
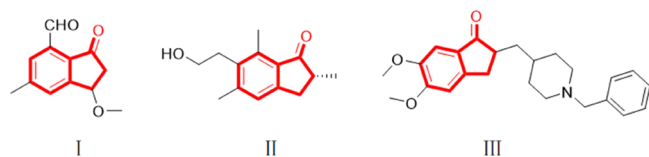
Figure 1. Compounds containing indanone.

In our previous studies,[25,26] we found that chalcone derivatives have good anti-TMV activity, so on this basis, we designed and synthesized them in order to obtain effective chalcone antiviral agents. By means of the active splicing principle, a series of chalcone derivatives were synthesized with indanone as the lead compound, and their anti-TMV activities were studied. Activity studies showed that most of the compounds had therapeutic, protective, and passivating activities against TMV, and some of them were better than NNM. The target compound **N2** with a higher activity was screened out, and its mechanism of anti-TMV was studied by a preliminary biological activity study, molecular docking, and a microscale thermophoresis test. The changes of malondialdehyde and defense enzymes in vivo were studied so as to provide a theoretical basis for the development of novel pesticides.

2. RESULTS AND DISCUSSION

2.1. Antiviral Activity of the Target Compounds N1−N20.
The anti-TMV activity of target compounds **N1−N20** was tested by the half-leaf dead spot method, and the results are shown in Table 1. When the test concentration was 500 μg/mL, there was a large gap between the therapeutic, protective, and passivation activities of **N2** and **N7**, which had good therapeutic activities, and the inhibition rates were 68.4 and 68.7%, respectively. They were better than those of NNM (61.3%). At the same concentration, the inhibition rates of **N1**,

N2, and **N10** on TMV were 72.2, 74.7, and 76.1%, respectively, which were significantly better than that of NNM (66.3%), showing better protective activities. The effect comparison was shown in Figure 2. The inhibition rates of **N6**
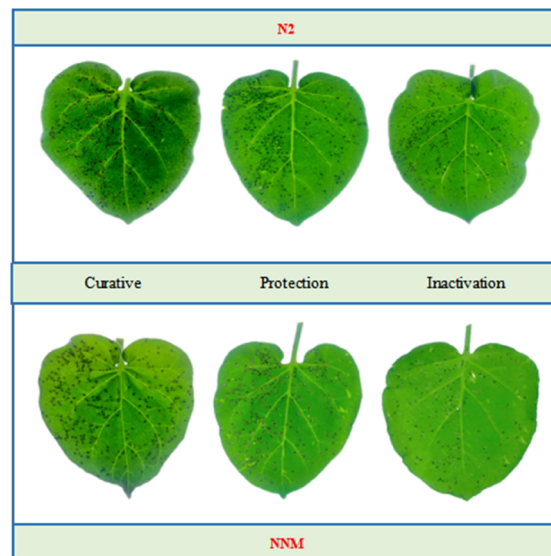

Figure 2. Tobacco leaf morphology effects of **N2** and NNM against TMV in vivo. The left side of each leaf was untreated with drug and the right side of each leaf was drug-treated.

and **N16** were 79.4 and 81.2%, respectively, slightly lower than that of NNM (93.2%). The preliminary test results showed that these compounds had good therapeutic and protective activities against TMV.

The EC_{50} values of **N1**, **N2**, **N7**, and **N10** with high activities were determined to further confirm their good antiviral

Table 1. Antiviral Activities (Concentration of 500 μg/mL) of the Target Compounds N1−N20 against TMV In Vivo[a]

compd.	O	R	inhibition rate[a] (%)		
			curative	protection	inactivation
N1	4	Ph	52.4 ± 6.9	72.2 ± 8.8	58.5 ± 7.4
N2	4	3-CH₃-Ph	68.4 ± 2.6	74.7 ± 5.7	42.0 ± 7.0
N3	4	4-CH₃-Ph	55.1 ± 8.1	61.3 ± 7.8	65.2 ± 8.3
N4	4	4-OCH₃-Ph	46.7 ± 1.8	67.2 ± 5.1	40.3 ± 6.7
N5	4	3-Cl-Ph	47.8 ± 7.4	56.0 ± 6.3	67.6 ± 5.1
N6	4	4-Cl-Ph	42.5 ± 1.8	54.8 ± 8.6	79.4 ± 8.4
N7	4	4-F-Ph	68.7 ± 8.0	65.5 ± 5.0	29.2 ± 7.7
N8	4	3,4-di-OCH₃-Ph	27.7 ± 2.5	65.5 ± 5.8	40.2 ± 5.0
N9	5	Ph	46.5 ± 8.6	65.7 ± 7.2	19.8 ± 0.2
N10	5	3-CH₃-Ph	58.0 ± 6.9	76.1 ± 5.6	65.7 ± 7.2
N11	5	4-CH₃-Ph	55.7 ± 8.2	49.2 ± 7.7	57.3 ± 5.0
N12	5	3-OCH₃-Ph	60.6 ± 5.3	43.1 ± 8.0	66.6 ± 4.6
N13	5	4-OCH₃-Ph	41.5 ± 9.7	37.0 ± 3.3	51.9 ± 2.4
N14	5	3-Cl-Ph	39.0 ± 8.6	29.1 ± 3.7	56.3 ± 3.2
N15	5	4-Cl-Ph	38.7 ± 1.9	21.5 ± 1.5	55.7 ± 0.8
N16	5	3-F-Ph	62.3 ± 8.9	45.6 ± 0.7	81.2 ± 5.2
N17	5	4-F-Ph	60.4 ± 4.9	34.2 ± 1.8	73.6 ± 8.7
N18	5	4-Br-Ph	37.2 ± 6.6	17.7 ± 2.9	63.1 ± 7.6
N19	5	3,4-di-OCH₃-Ph	39.4 ± 8.0	46.3 ± 5.8	70.1 ± 7.5
N20	5	furan-2-Ph	41.2 ± 1.3	41.0 ± 7.7	65.7 ± 6.2
NNM			61.3 ± 1.2	66.3 ± 6.6	93.2 ± 4.7

[a]Average of three replicates.

Table 2. EC$_{50}$ Values of Several Target Compounds and NNM against TMV

	compd.	O	R	toxic regression equation	r^2	EC$_{50}$/(μg/mL)
curative activity	**N2**	4	3-CH$_3$-Ph	$y = 0.9259x + 3.2879$	0.9873	70.7
	N7	4	4-F-Ph	$y = 0.6544x + 3.7216$	0.9679	89.9
	NNM			$y = 0.6159x + 3.6453$	0.9426	158.3
protection activity	**N1**	4	Ph	$y = 1.0654x + 2.7713$	0.9522	123.6
	N2	4	3-CH$_3$-Ph	$y = 0.6551x + 3.8315$	0.9721	60.8
	N10	5	3-CH$_3$-Ph	$y = 1.0552x + 2.8049$	0.9891	120.3
	NNM			$y = 0.8241x + 3.1503$	0.9848	175.6
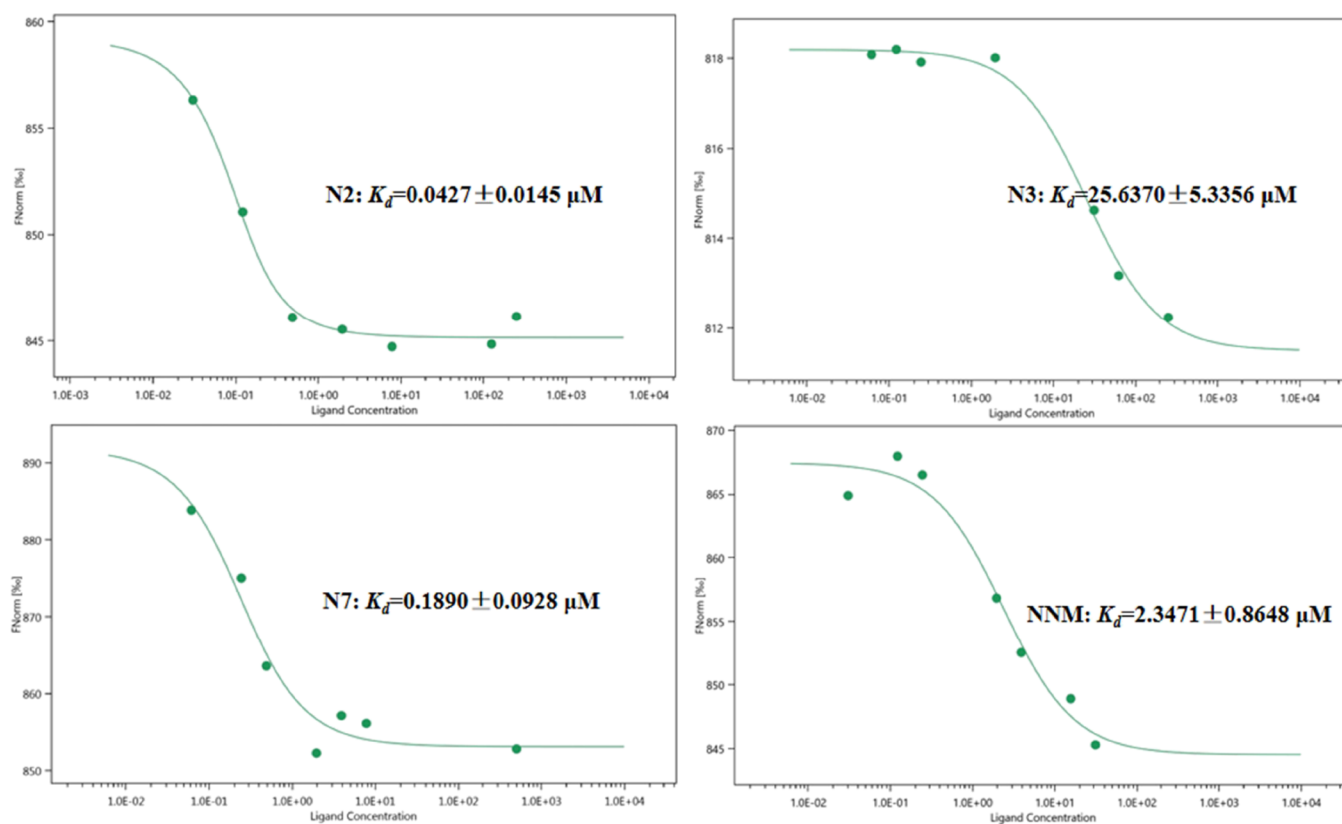
**Figure 3.** MST of compounds **N2**, **N3**, **N7**, and NNM to TMV-CP.

activities (Table 2). The EC$_{50}$ values of **N2** and **N7** against TMV were 70.7 and 89.9 μg/mL, respectively, which were better than that of NNM (158.3 μg/mL). In comparison, the EC$_{50}$ values of **N1**, **N2**, and **N10** were 123.6, 60.8, and 120.3 μg/mL, respectively, which were significantly superior to the EC$_{50}$ value of NNM (175.6 μg/mL). It can be seen that the protective activities of **N1**, **N2**, and **N10** were better than that of NNM. In particular, the therapeutic and protective activities of **N2** were significantly better than those of NNM, and it had good antiviral activity, which was worthy of further research.

2.2. Structure−Activity Relationship. Most of the target compounds **N1−N20** had better antiviral activities than NNM. The therapeutic, protective, and passivating activities vary according to their substituent and positions. As can be seen from Table 1, when R was 3-CH$_3$-Ph (**N2**) and 4-CH$_3$-Ph (**N3**), the therapeutic effect on TMV significantly enhanced, and the inhibition rates were 64.8 and 55.1%, respectively, which were better than the inhibition rate when R was Ph (**N1**) (52.4%), so the therapeutic activity was better when R was an electron donor group. Taking 3-CH$_3$-Ph (**N2**) and 4-CH$_3$-Ph (**N3**) as examples, the corresponding target compound **N2** had better therapeutic activity than **N3**. It

can be seen that the therapeutic, protective, and passivating activities of substituents in the *meta*-position were higher than those in the *para*-position, and the therapeutic, protective, and passivating activities of **N1−N20** followed this rule basically.

2.3. Microscale Thermophoresis. Microscale thermophoresis (MST) was used to investigate the binding ability of target compounds **N2**, **N7**, and NNM to the TMV coat protein (TMV-CP). The MST test results are shown in Figure 3. The K_d values of **N2** and **N7** were 0.0427 $\pm$ 0.0145 and 0.1890 $\pm$ 0.0928 μM, respectively, which were better than that of NNM (2.3471 $\pm$ 0.8648 μM). In summary, **N2** and **N7** were more potent than NNM in binding to TMV-CP, suggesting that **N2** and **N7** were more potent than the controlled drug.

2.4. Molecular Docking. Molecular docking experiments of **N2** and NNM with TMV-CP were performed to simulate the interaction between the drug molecules and TMV-CP. As shown in Figure 4, there is a hydrogen bond interaction between **N2** and ARG-341 with a bond length of 3.08 Å. There was a hydrogen bond between NNM and SER-138 and ASP-66 with bond lengths of 4.29 and 3.72 Å, respectively. Although the docking of NNM with TMV-CP produced more
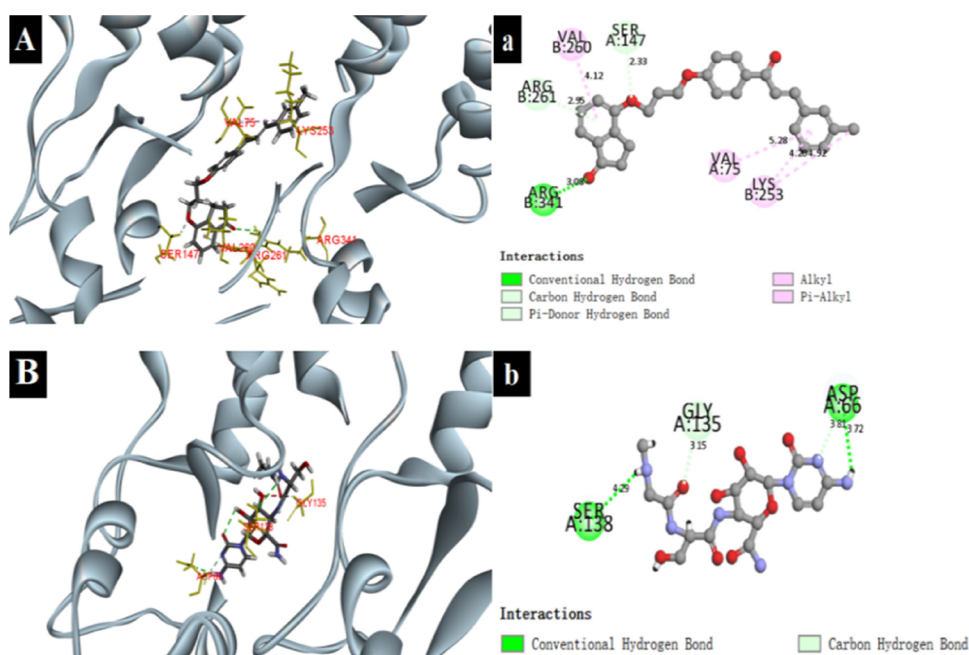
Figure 4. Molecular docking of compounds **N2** (A, a) and NNM (B, b) to TMV-CP.

hydrogen bonds than **N2**, the hydrogen bond length of **N2** was shorter and its binding was closer. Compound **N2** was bound to ARG-261 and SER-147 through a C−H bond with bond lengths of 2.95 and 2.33 Å, respectively, and bound to VAL-260, VAL-75, and LYS-253 through a π-alkyl hydrophobic bond with bond lengths of 4.12, 5.28, and 4.92 Å, respectively. NNM binds to GLY-135 via a C−H bond with a bond length of 3.15 Å. In conclusion, **N2** binds to TMV-CP through more bonds and their interaction forces are stronger.

2.5. Malondialdehyde Content. As shown in Figure 5, the content of malondialdehyde (MDA) in leaves was
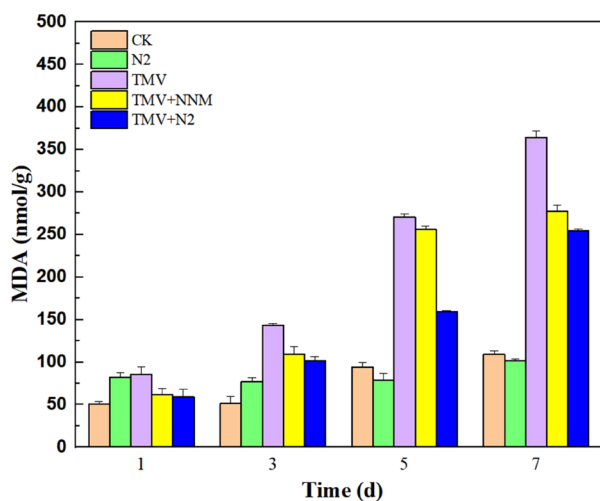
Figure 5. Changes in the MDA content in tobacco after compound **N2** treatment.

measured after 1, 3, 5, and 7 days of treatment. The accumulation of reactive oxygen species induced membrane lipid peroxidation when plants suffered from various environmental stresses in their life cycle. The main products of membrane lipid peroxidation are MDA, etc. Therefore, the degree of membrane lipid peroxidation, the degree of

membrane damage, and the stress resistance of plants can be measured by measuring the MDA content. With the passage of time, the MDA content in leaves treated with CK increased mainly because of environmental adversity and leaf senescence. The content of MDA in the leaves treated with **N2** continued to increase, but the content of MDA in the leaves after 5−7 days was relatively lower than that of the untreated leaves because **N2** could cause adverse effects in a negative environment. The content of MDA in leaves treated with TMV increased significantly with time, which fully reflected the destruction of leaves caused by TMV. The MDA content of **TMV + N2** and **TMV + NNM** treatment increased, but the rapid damage of the TMV virus to leaves was significantly inhibited. The MDA content of **TMV + N2** treatment was lower than that of **TMV + NNM** treatment from the beginning to end. It could be seen that the activity of the target compound **N2** against **TMV** was significantly better than that of the control drug NNM.

2.6. Activities of the Defense Enzyme. *2.6.1. Superoxide Dismutase Assay.* Figure 6 shows the changes in the superoxide dismutase (SOD) content in leaves after treatment with the target compound **N2**. The SOD content in leaves with **TMV + N2** treatment increased gradually from 1 to 7 days, which was significantly better than that of leaves treated with NNM. Compared with the SOD content of TMV treatment and **TMV + N2** treatment, it can be seen that the SOD content of **N2** treatment is significantly better than that of TMV treatment, so **N2** can induce SOD production in leaves and improve the antivirus ability of leaves.

2.6.2. Peroxidase Determination. The changes in the peroxidase (POD) content in leaves treated with **N2** and NNM for 1, 3, 5, and 7 days were shown in Figure 7. The POD content in leaves treated with TMV gradually increased over time but the content was less than that before 7 days. The content of POD in **TMV + NNM** treatment increased significantly, and the difference was more obvious in 1 day. That was to say, NNM treatment induced the production of defense enzymes faster, while the content of POD in **TMV +**
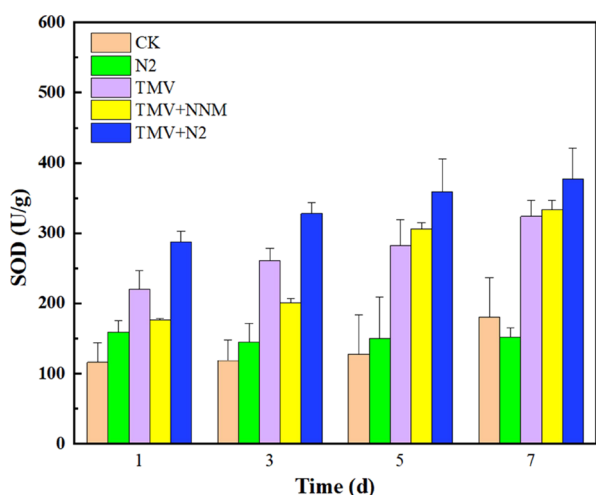
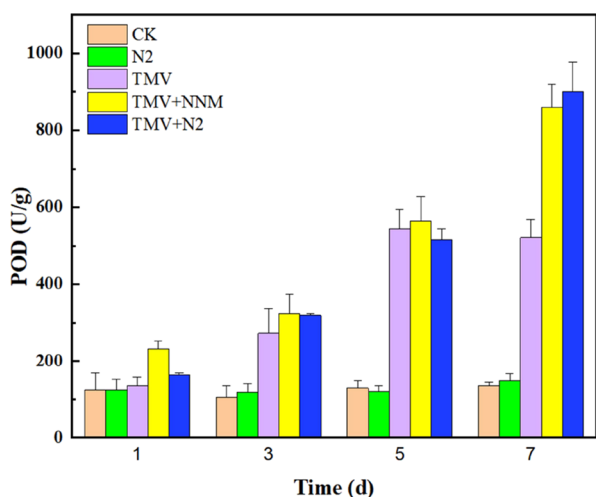**Figure 6.** Changes in the SOD content in tobacco after compound **N2** treatment.

Figure 7. Changes in the POD content in tobacco after compound **N2** treatment.

N2 treatment increased within 1, 3, and 5 days, but the increase range was more than that of NNM until 7 days when the POD content exceeded that of NNM. It was concluded that **N2** could induce the production of defense enzymes and the induction effect was better in 7 days.
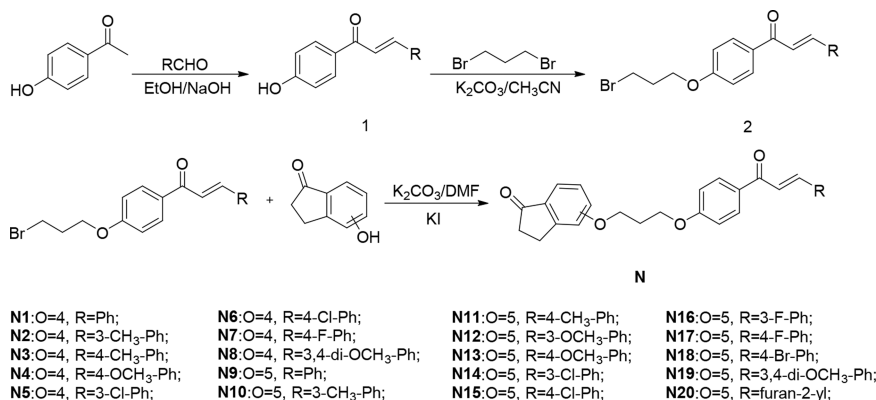
3. CONCLUSIONS

In summary, the derivatives of chalcone containing indanone showed good antiviral activity. The therapeutic and protective activities of **N2** and **N7** were better than those of the control drug NNM, which was confirmed by the K_d values obtained from MST. The determined MDA content also reflected the activity of **N2** against TMV. The results of defense enzyme tests also showed that **N2** promoted the production of defense enzymes. That was to say, with the help of **N2**, tobacco further activated the autoimmune response of tobacco, improving its disease resistance and thus making it more effective against TMV. Therefore, the design and synthesis of chalcone derivatives containing indanone provide value for the development of new antiviral agents.

4. MATERIALS AND METHODS

4.1. Instruments and Chemicals. The melting point was measured by using an X-4 digital micro-melting point tester (Beijing Tektronix Instruments) without correction. The ^{1}H, ^{13}C, and ^{19}F nuclear magnetic resonance (NMR) spectra of target compounds were characterized by using a JEOL ECX500 500 MHz NMR instrument (JEOL, Japan). High-resolution mass spectrometry (HRMS) was performed using an LC−MS 1100/MSD LC−MS/MS system (Agilent, USA). All chemicals were of analytical grade and purchased from Tianjin Zhiyuan Company. MDA and defense enzyme test kits were purchased from Solarbio.

4.2. Synthesis. *4.2.1. General Synthesis Procedure for Intermediates 1 and 2.* Hydroxyacetophenone (20 mmol) and aldehydes with different substituents (24 mmol) were added to a three-necked flask followed by (30 mL) ethanol to fully dissolve the reactants and 50 mL of 5% NaOH solution, according to ref 27. Magnetic stirring was carried out at room temperature for 12 h until the reaction was complete. Thin-layer chromatography (TLC) was employed to monitor the raw materials. When the raw material point disappeared, the reaction system was poured into an ice−water mixture. Its pH was adjusted until it was about 5 in the beaker when measured. In **intermediate 1**, some yellow solids appeared at the bottom of the flask. The **intermediate 1** (10 mmol) and potassium carbonate (25 mmol) were dissolved in 30 mL of acetonitrile and heated at 80 °C for 1 h. Then, dibromopropane (50 mmol) was added to the reaction system, and heating was continued until the reaction system was white. It was poured into water for dispersion, and a white solid was precipitated,

Scheme 1. Synthetic Route of Target Compounds N1−N20

N1:O=4, R=Ph;
N2:O=4, R=3-CH₃-Ph;
N3:O=4, R=4-CH₃-Ph;
N4:O=4, R=4-OCH₃-Ph;
N5:O=4, R=3-Cl-Ph;

N6:O=4, R=4-Cl-Ph;
N7:O=4, R=4-F-Ph;
N8:O=4, R=3,4-di-OCH₃-Ph;
N9:O=5, R=Ph;
N10:O=5, R=3-CH₃-Ph;

N11:O=5, R=4-CH₃-Ph;
N12:O=5, R=3-OCH₃-Ph;
N13:O=5, R=4-OCH₃-Ph;
N14:O=5, R=3-Cl-Ph;
N15:O=5, R=4-Cl-Ph;

N16:O=5, R=3-F-Ph;
N17:O=5, R=4-F-Ph;
N18:O=5, R=4-Br-Ph;
N19:O=5, R=3,4-di-OCH₃-Ph;
N20:O=5, R=furan-2-yl;

extracted and evaporated under a reduced pressure, dried, and then obtained **intermediate 2**.

4.2.2. General Synthesis of Target Compounds N1−N20. Hydroxyindanone (10 mmol), potassium carbonate (25 mmol), and a catalytic dose of iodomethane were added to a round-bottom flask, and 10 mL of *N,N*-dimethylformamide was added and stirred until it dissolved. After heating to 85 °C, **intermediate 2** (12 mmol) was added after 1 h while being monitoring by TLC until the raw materials disappeared. At the end of the reaction, the whole reaction system was poured into water for dispersion, extracted and filtered under a reduced pressure, and dried to obtain the crude products. They were separated and purified by silica gel column chromatography (ethyl acetate/petroleum ether = 1:5). The synthetic route of **N1−N20** is shown in Scheme 1.

4.3. Anti-TMV Bioassay. The therapeutic, protective, and passivating activities of target compounds **N1−N20** against TMV were tested at a concentration of 500 μg/mL using the half-leaf dead spot method as described in the literature.[28] To determine the antiviral activity of the target compounds, the commercially available 8% NNM was used as a control. The treated tobacco plants were cultured in a greenhouse (28 °C) for 2 days, and the number of spots on the left and right sides was counted when spots appeared on the leaves, and the inhibition rate was calculated. Three parallel experiments were conducted for each drug.

$$\text{inhibition rate (\%)} = \frac{A_1 - A_2}{A_1} \times 100\%$$

where A_1 is the number of spots under a blank control and A_2 is the number of spots under treatment control.

4.4. MST Experiment. To further study the affinity between the target compound and the TMV-CP, the NHS-647 dye was added to the purified TMV protein according to ref 29, incubated, and eluted with column B. Sixteen samples with a gradient concentration were prepared, and 10 μL of each sample was introduced into the capillary for the MST experiment. The molecules bound to the dye moved by forcing the heat surge, and the measured K_d value can accurately reflect the interaction among the molecules.

4.5. Molecular Docking. Dock ligands in Discovery Studio were used for molecular docking, which simulated the binding mode and affinity of ligands and receptors through the interaction between them. The coat protein of TMV was coded as 1EI7 according to the reference and retrieved from the official website of Protein Data Bank in Europe.[30] After the homology comparison with the CP sequence of TMV, the protein template was imported into Discovery Studio software for clean protein backup. A 3D model of the compound structure was constructed and optimized, and then the molecular docking was performed with the treated protein template to simulate the binding ability between the compound and the protein.

4.6. Determination of the MDA Content. An eight-leaf tobacco with consistent growth and healthy growth was selected. Five treatments were carried out, namely, blank control (CK), target compound **N2** (drug control), **TMV**, **TMV + NNM**, and **TMV + N2**, with three plants in each treatment. The samples were picked at intervals of 1, 3, 5, and 7 days. The tobacco leaves were picked and placed in a mortar, placed into liquid nitrogen, ground to powder, divided into 10 mL centrifuge tubes, and stored in a refrigerator at −80 ° C.

The accumulation of reactive oxygen species induces membrane lipid peroxidation when plants suffer from various environmental stresses in their life cycle. The main products of membrane lipid peroxidation are MDA and so on. Therefore, the degree of membrane lipid peroxidation, the degree of membrane damage, and the stress resistance of tobacco leaves treated with **TMV + N2** can be measured by the content of MDA. The MDA was determined by the method of thiobarbituric acid.[31] The absorbance of each sample at 532 and 600 nm was measured using a microplate reader, and the MDA content was calculated according to the following formula. Origin software was used for processing the data.

$$\Delta A532 = A532_{\text{determination}} - A532_{\text{blank}}$$

$$\Delta A600 = A600_{\text{determination}} - A600_{\text{blank}}$$

$$\Delta A = \Delta A532 - \Delta A600$$

MDA content (nmol/g)

$$= \frac{[\Delta A \times V_a \div (\varepsilon \times d) \times 10^9]}{W \times V_b \div V_c} \times F$$

where V_a is the total volume of the reaction system; ε is the MDA molar absorbance coefficient, 1.55×10^5 L/mol/cm; d is the optical diameter of a 96-well plate; W is the sample quality, g; V_b is the added sample volume; V_c is the added volume of extraction liquid, mL; and F is the dilution factor.

4.7. Determination of the Defense Enzyme Activity. The sample preparation method was the same as that in the MDA content determination.

4.7.1. SOD Assay. SOD is a metalloenzyme that widely exists in animals, plants, and microorganisms. It can catalyze the dismutation reaction of a superoxide radical ($O^{2−}$) in an organism and it is the natural eliminator of $O^{2−}$ in the body. Thus, scavenging $O^{2−}$ plays an extremely important role in the self-protection system of the organism. It also plays an important role in the immune system. The absorbance value of blue formazan produced by the reduction of nitroblue tetrazolium (NBT) was used to determine the SOD content.[32] The absorbance of each tube was measured at 560 nm, and 50% inhibition of the photochemical reduction of NBT was taken as 1 unit of enzyme activity U/g.

4.7.2. POD Determination. The role of POD is mainly to hydrolyze hydrogen peroxide. Hydrogen peroxide (H_2O_2) is a cytotoxic substance produced in the redox reaction catalyzed by oxidases. Both oxidases and catalase exist in peroxisomes, thereby protecting cells and eliminating the toxicity of hydrogen peroxide and phenol, amines, aldehydes, and benzene. POD was used to oxidize guaiacol in the presence of hydrogen peroxide to produce a brown substance,[33] and its absorbance value at 470 nm was measured to calculate the POD content in leaves.

■ ASSOCIATED CONTENT

Ⓢ Supporting Information

The Supporting Information is available free of charge at https://pubs.acs.org/doi/10.1021/acsomega.2c07071.

> Characterization data , experimental details, spectrogram data of the target compounds **N1−N20**, and ^{1}H, ^{13}C, and ^{19}F NMR spectra and HRMS spectra of title compounds (PDF)

■ AUTHOR INFORMATION

Corresponding Author

Wei Xue − *State Key Laboratory Breeding Base of Green Pesticide and Agricultural Bioengineering; Key Laboratory of Green Pesticide and Agricultural Bioengineering, Ministry of Education; Research and Development Center for Fine Chemicals, Guizhou University, Guiyang 550025, P.R. China;* ● orcid.org/0000-0003-4471-5414; Phone: +86-851-88292090; Email: wxue@gzu.edu.cn; Fax: +86-851-88292090

Authors

Nan Sun − *State Key Laboratory Breeding Base of Green Pesticide and Agricultural Bioengineering; Key Laboratory of Green Pesticide and Agricultural Bioengineering, Ministry of Education; Research and Development Center for Fine Chemicals, Guizhou University, Guiyang 550025, P.R. China*

Chenyu Gong − *State Key Laboratory Breeding Base of Green Pesticide and Agricultural Bioengineering; Key Laboratory of Green Pesticide and Agricultural Bioengineering, Ministry of Education; Research and Development Center for Fine Chemicals, Guizhou University, Guiyang 550025, P.R. China*

Yuanxiang Zhou − *State Key Laboratory Breeding Base of Green Pesticide and Agricultural Bioengineering; Key Laboratory of Green Pesticide and Agricultural Bioengineering, Ministry of Education; Research and Development Center for Fine Chemicals, Guizhou University, Guiyang 550025, P.R. China*

Yuanquan Zhang − *State Key Laboratory Breeding Base of Green Pesticide and Agricultural Bioengineering; Key Laboratory of Green Pesticide and Agricultural Bioengineering, Ministry of Education; Research and Development Center for Fine Chemicals, Guizhou University, Guiyang 550025, P.R. China*

Nian Zhang − *State Key Laboratory Breeding Base of Green Pesticide and Agricultural Bioengineering; Key Laboratory of Green Pesticide and Agricultural Bioengineering, Ministry of Education; Research and Development Center for Fine Chemicals, Guizhou University, Guiyang 550025, P.R. China*

Li Xing − *State Key Laboratory Breeding Base of Green Pesticide and Agricultural Bioengineering; Key Laboratory of Green Pesticide and Agricultural Bioengineering, Ministry of Education; Research and Development Center for Fine Chemicals, Guizhou University, Guiyang 550025, P.R. China*

Complete contact information is available at:
https://pubs.acs.org/10.1021/acsomega.2c07071

Notes

The authors declare no competing financial interest.

■ REFERENCES

(1) Zhou, X.; Ye, Y. Q.; Liu, S. S.; Shao, W. B.; Liu, L. W.; Yang, S.; Wu, Z. B. Design, synthesis and anti-TMV activity of novel α-aminophosphonate derivatives containing a chalcone moiety that induce resistance against plant disease and target the TMV coat protein. *Pestic. Biochem. Phys.* **2021**, *172*, No. 104749.

(2) Basit, A.; Farhan, M.; Mo, W. D.; Ding, H. X.; Ikram, M.; Farooq, T.; Ahmed, S.; Yang, Z. F.; Wang, Y.; Hashem, M.; Alamri, S.; Bashir, M. A.; El-Zohri, M. Enhancement of resistance by poultry manure and plant hormones (salicylic acid & citric acid) against tobacco mosaic virus. *Saudi J. Biol. Sci.* **2021**, *28*, 3526−3533.

(3) Li, Y. F.; Jiao, Y. B.; Shi, J.; Xie, J. J.; Yin, J.; Zhao, X. X.; Chen, H. M. BLB8, an antiviral protein from *Brevibacillus laterosporus* strain B8, inhibits Tobacco mosaic virus infection by triggering immune response in tobacco. *Pest Manage. Sci.* **2021**, *77*, 4383−4392.

(4) Zhao, L.; Feng, C. H.; Wu, K.; Chen, W. B.; Chen, Y. J.; Hao, X. G.; Wu, Y. F. Advances and prospects in biogenic substances against plant virus: A review. *Pestic. Biochem. Phys.* **2017**, *135*, 15−26.

(5) Wang, D. N.; Liang, J.; Zhang, J.; Wang, Y. F.; Chai, X. Natural chalcones in chinese materia medica: licorice. *Evidence-Based Complementary Altern. Med.* **2020**, *2020*, 14.

(6) Du, C.; Hou, J.; Wang, C.; Zhang, M. Y.; Zheng, Y. J.; Yang, G.; Hu, Y. L. Effects of safflower yellow on cholesterol levels in serum and brain tissue of APP/PS1 mice. *Metab. Brain Dis.* **2021**, *36*, 557−569.

(7) Zhang, M. R.; Jiang, K.; Yang, J. L.; Shi, Y. P. Flavonoids as key bioactive components of Oxytropis falcata bunge, a traditional anti-inflammatory and analgesic Tibetan medicine. *Nat. Prod. Res.* **2020**, *34*, 3335−3352.

(8) Nuti, E.; Bassani, B.; Camodeca, C.; Rosalia, L.; Cantelmo, A. R.; Gallo, C.; Baci, D.; Bruno, A.; Orlandini, E.; Nencetti, S.; Noonan, D. M.; Albini, A.; Rossello, A. synthesis and antiangiogenic activity study of new hop chalcone Xanthohumol analogues. *Eur. J. Med. Chem.* **2017**, *138*, 890−899.

(9) Mustafa, M.; Mostafa, Y. A. A facile synthesis, drug-likeness, and in silico molecular docking of certain new azidosulfonamide-chalcones and their in vitro antimicrobial activity. *Monatsh. Chem.* **2020**, *151*, 417−427.

(10) Fu, Y.; Liu, D.; Zeng, H. N.; Ren, X. L.; Song, B. A.; Hu, D. Y.; Gan, X. H. New chalcone derivatives: synthesis, antiviral activity and mechanism of action. *RSC Adv.* **2020**, *10*, 24483−24490.

(11) Zulu, A. I.; Oderinlo, O. O.; Kruger, C.; Isaacs, M.; Hoppe, H. C.; Smith, V. J.; Veale, C. G. L.; Khanye, S. D. Synthesis, structure and in vitro anti-trypanosomal activity of non-toxic arylpyrrole-based chalcone derivatives. *Molecules* **2020**, *25*, 1668.

(12) Tang, Y. L.; Zheng, X.; Qi, Y.; Pu, X. J.; Liu, B.; Zhang, X.; Li, X. S.; Xiao, W. L.; Wan, C. P.; Mao, Z. W. Synthesis and anti-inflammatory evaluation of new chalcone derivatives bearing bispiperazine linker as IL-1β inhibitors. *Bioorg. Chem.* **2020**, *98*, No. 103748.

(13) Li, K.; Zhao, S.; Long, J.; Su, J.; Wu, L. S.; Tao, J.; Zhou, J. D.; Zhang, J. L.; Chen, X.; Peng, C. A novel chalcone derivative has antitumor activity in melanoma by inducing DNA damage through the upregulation of ROS products. *Cancer Cell. Int.* **2020**, *20*, 36.

(14) Sivakumar, P. M.; Prabhakar, P. K.; Doble, M. Synthesis, antioxidant evaluation, and quantitative structure−activity relationship studies of chalcones. *Med. Chem. Res.* **2011**, *20*, 482−492.

(15) Koyii, M. M.; Gezegen, H.; Taslimi, P. Synthesis, characterization, and biological studies of chalcone derivatives containing Schiff bases: Synthetic derivatives for the treatment of epilepsy and Alzheimer's disease. *Arch. Pharmacal Res.* **2020**, *353*, No. 2000202.

(16) Chen, Z. H.; Zheng, C. J.; Sun, L. P.; Piao, H. R. Synthesis of new chalcone derivatives containing a rhodanine-3-acetic acid moiety with potential anti-bacterial activity. *Eur. J. Med. Chem.* **2010**, *45*, 5739−5743.

(17) Nagle, D. G.; Zhou, Y. D.; Park, P. U.; Paul, V. J.; Rajbhandari, I.; Duncan, C. J. G.; Pasco, D. S. A new indanone from the marine cyanobacterium Lyngbya majuscula that inhibits hypoxia-induced activation of the VEGF promoter in Hep3B cells. *J. Nat. Prod.* **2000**, *63*, 1431−1433.

(18) Patil, S. A.; Patil, R.; Patil, S. A. Recent developments in biological activities of indanones. *Eur. J. Med. Chem.* **2017**, *138*, 182−198.

(19) Finkieisztein, L. M.; Castro, E. F.; Fabian, L. E.; Moltrasio, G. Y.; Campos, R. H.; Cavallaro, L. V.; Moglioni, A. G. New 1-indanone thiosemicarbazone derivatives active against BVDV. *Eur. J. Chem.* **2008**, *43*, 1767−1773.

(20) Patil, S. A.; Patil, V.; Patil, R.; Beaman, K.; Patil, S. A. Identification of novel 5,6-dimethoxyindan-1-one derivatives as antiviral agents. *Med. Chem.* **2017**, *13*, 787−795.

(21) Costanzo, P.; Cariati, L.; Desiderio, D.; Sgammato, R.; Lamberti, A.; Arcone, R.; Salerno, R.; Nardi, M.; Masullo, M.; Oliverio, M. Design, synthesis, and evaluation of donepezil-like compounds as AChE and BACE-1 inhibitors. *ACS Med. Chem. Lett.* **2016**, *7*, 470−475.

(22) Lv, P. C.; Elsayed, M. S.; Agama, K.; Marchand, C.; Pommier, Y.; Cushman, M. Design, synthesis, and biological evaluation of potential prodrugs related to the experimental anticancer agent indotecan (LMP400). *J. Med. Chem.* **2016**, *59*, 4890−4899.

(23) Wu, M.; Li, L.; Feng, A. Z.; Su, B.; Liang, D. M.; Liu, Y. X.; Wang, Q. M. First total synthesis of Papilistatin. *Org. Biomol. Chem.* **2011**, *9*, 2539−2542.

(24) Van der Zee, E. A.; Platt, B.; Riedel, G. Acetylcholine: future research and perspectives. *Behav. Brain Res.* **2011**, *211*, 583−586.

(25) Xia, R. J.; Guo, T.; He, J.; Chen, M.; Su, S. J.; Jiang, S. C.; Tang, X.; Chen, Y.; Xue, W. Antimicrobial evaluation and action mechanism of chalcone derivatives containing quinoxaline moiety. *Monatsh. Chem.* **2019**, *150*, 1325−1334.

(26) Tang, X.; Su, S. J.; Chen, M.; He, J.; Xia, R. J.; Guo, T.; Chen, Y.; Zhang, C.; Wang, J.; Xue, W. Novel chalcone derivatives containing a 1,2,4-triazine moiety: design, synthesis, antibacterial and antiviral activities. *RSC Adv.* **2019**, *9*, 6011−6020.

(27) Guo, T.; Xia, R. J.; Chen, M.; He, J.; Su, S. J.; Liu, L. W.; Li, X. Y.; Xue, W. Biological activity evaluation and action mechanism of chalcone derivatives containing thiophene sulfonate. *RSC Adv.* **2019**, *9*, 24942−24950.

(28) Zhang, J.; He, F. C.; Chen, J. X.; Wang, Y. J.; Yang, Y. Y.; Hu, D. Y.; Song, B. A. Purine nucleoside derivatives containing a sulfa ethylamine moiety: design, synthesis, antiviral activity, and mechanism. *J. Agric. Food Chem.* **2021**, *69*, 5575−5582.

(29) Wang, Y. J.; He, F. C.; Wu, S. K.; Luo, Y. Q.; Wu, R.; Hu, D. Y.; Song, B. A. Design, synthesis, anti-TMV activity, and preliminary mechanism of cinnamic acid derivatives containing dithioacetal moiety. *Pestic. Biochem. Phys.* **2020**, *164*, 115−121.

(30) Peng, F.; Liu, T. T.; Wang, Q. F.; Liu, F.; Cao, X.; Yang, J. S.; Liu, L. W.; Xie, C. W.; Xue, W. Antibacterial and antiviral activities of 1,3,4-oxadiazole thioether 4H-chromen-4-one derivatives. *J. Agric. Food Chem.* **2021**, *69*, 11085−11094.

(31) Soares, F. A. C.; Kretzmann Filho, V.; Beretta, B. F. S.; Linden, T. S.; Pöppl, A. G.; González, F. H. D. Thiobarbituric acid reactive substances in dogs with spontaneous hypercortisolism. *Domest. Anim. Endocrinol.* **2021**, *77*, No. 106634.

(32) Bhatia, K.; Mal, G.; Bhar, R.; Jyoti; Attri, C.; Seth, A. Purification and characterization of thermostable superoxide dismutase from Anoxybacillus gonensis KA 55 MTCC 12684. *Int. J. Biol. Macromol.* **2018**, *117*, 1133−1139.

(33) Huyskens-Keil, S.; Eichholz-Dündar, I.; Hassenberg, K.; Herppich, W. B. Impact of light quality (white, red, blue light and UV-C irradiation) on changes in anthocyanin content and dynamics of PAL and POD activities in apical and basal spear sections of white asparagus after harvest. *Postharvest Biol. Technol.* **2020**, *161*, No. 111069.